Measurements of $\sin 2\beta$ and ϕ_s with the full LHCb Run 1 & 2 data sample

Vukan Jevtic (TU Dortmund), Peilian Li (CERN)
On behalf of the LHCb collaboration

June 13, 2023
LHC Seminar

CP-violation history

1957

C. Yang
T. D. Lee

1980

J. Cronin
V. Fitch

2008

Y. Nambu
M. Kobayashi
T. Maskawa

1956
Discovery of parity violation (Wu experiment)

1964
CP violation in mixing is discovered in neutral kaon decays by Cronin, Fitch et al. at Brookhaven

1987
Observation of $B^0\overline{B}^0$ mixing (ARGUS)

1999
First observation of CPV in decays (Na48& KTeV)

2001
Discovery of time-dependent *CP* violation in B^0 meson decays by BaBar and Belle

2006
Observation of B_s^0-$\overline{B}_s^0$ oscillation (CDF)

2019
Observation of CPV in D^0 decays (LHCb)

2020
Observation of TDCPV in B_s^0 decays (LHCb)

CKM mechanism

SM charged current interaction

$$\mathcal{L}_{W^\pm} = \frac{g}{\sqrt{2}} \left(\overline{u_L} \gamma^\mu W_\mu^+ V_{\text{CKM}} d_L + \overline{d_L} \gamma^\mu W_\mu^- V_{\text{CKM}}^\dagger u_L \right)$$

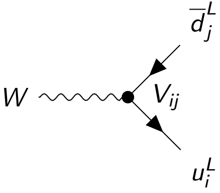

$$V_{\text{CKM}} = \begin{pmatrix} V_{ud} & V_{us} & V_{ub} \\ V_{cd} & V_{cs} & V_{cb} \\ V_{td} & V_{ts} & V_{tb} \end{pmatrix}$$

- The unitary CKM matrix V_{CKM} introduces tree-level couplings between up and down-type quarks
- 3 free parameters + CP violating phase δ
- V_{CKM} unitarity tested by over-constraining CKM parameters

CKM measurements through the years

One of unitarity conditions: $V_{ud}V_{ub}^* + V_{cd}V_{cb}^* + V_{td}V_{tb}^* = 0$

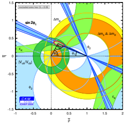

2004

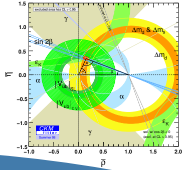

2008

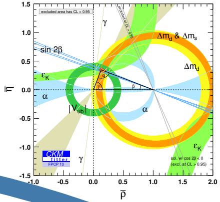

2013

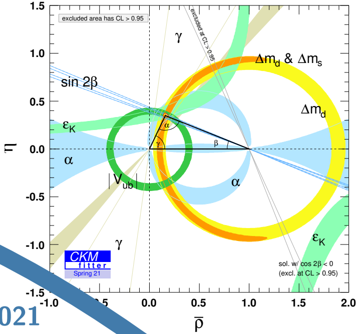

2021

Wolfenstein parametrization

Scaled apex coordinates

$$V_{\rm CKM} = \begin{pmatrix} 1-\lambda^2/2 & \lambda & A\lambda^3(\rho - i\eta) \\ -\lambda & 1-\lambda^2/2 & A\lambda^2 \\ A\lambda^3(1-\rho-i\eta) & -A\lambda^2 & 1 \end{pmatrix} + \mathcal{O}(\lambda^4)$$

$\lambda \approx 0.224$

2023

CKM measurements through the years

One of unitarity conditions: $V_{ud} V_{ub}^* + V_{cd} V_{cb}^* + V_{td} V_{tb}^* = 0$

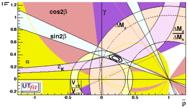

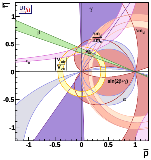

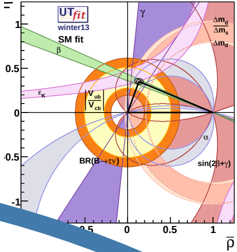

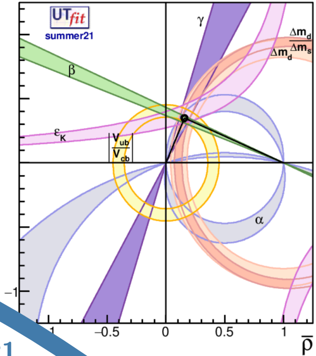

2004

2011

2013

2021

2023

Wolfenstein parametrization

Scaled apex coordinates

$$V_{\mathrm{CKM}} = \begin{pmatrix} 1-\lambda^2/2 & \lambda & A\lambda^3(\rho - i\eta) \\ -\lambda & 1-\lambda^2/2 & A\lambda^2 \\ A\lambda^3(1-\rho-i\eta) & -A\lambda^2 & 1 \end{pmatrix} + \mathcal{O}(\lambda^4)$$

$\lambda \approx 0.224$

Neutral B meson oscillation

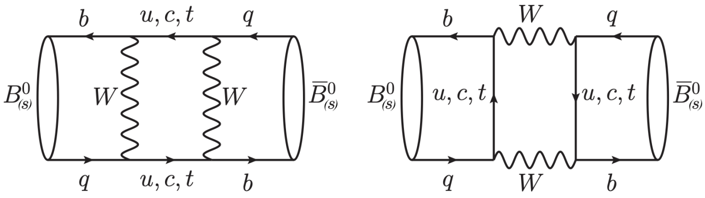

Mixing and decay can be described by Schrödinger-like equation

$$i\frac{d}{dt}\begin{pmatrix} B \\ \overline{B} \end{pmatrix} = \tilde{\mathbf{H}}\begin{pmatrix} B \\ \overline{B} \end{pmatrix} = \begin{bmatrix} m - \frac{i}{2}\Gamma & m_{12} - \frac{i}{2}\Gamma_{12} \\ m_{12}^* - \frac{i}{2}\Gamma_{12}^* & m - \frac{i}{2}\Gamma \end{bmatrix}\begin{pmatrix} B \\ \overline{B} \end{pmatrix}$$

describing the decay and time-dependent mixing. The resulting decay rates of initial B and $\overline{B}$ are

$$|\langle f|H|B_{(s)}\rangle|^2 = \frac{1}{2}e^{-\Gamma t}|A_f|^2\Big\{\cosh\left(\frac{\Delta\Gamma}{2}t\right) + \boldsymbol{A_{\Delta\Gamma}}\sinh\left(\frac{\Delta\Gamma}{2}t\right) + \boldsymbol{C}\cos(\Delta m t) - \boldsymbol{S}\sin(\Delta m t)\Big\}$$

Opportunities for probing for new physics

- NP short-distance contributions can influence mixing
  $m_{12}^{q} = m_{12}^{\mathrm{SM},q} \cdot \Delta_{q}^{\mathrm{NP}}$
  PRD 86(2012)033008
- Through B mixing, NP energy scales of up to 20 TeV for tree level NP or 2 TeV for NP in loops can be probed
  PRD 89 (2014) 033016

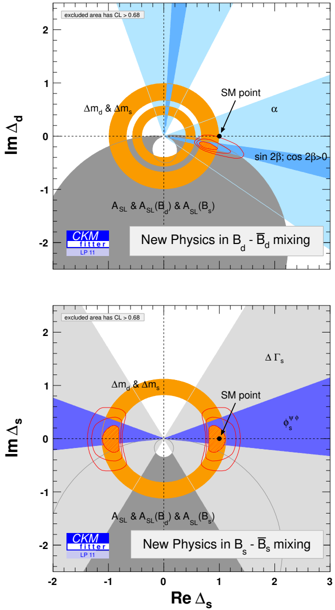

CP violation

CP-violating nature of weak interaction has multiple manifestations

CP violation in mixing

Unequal transition probabilities between flavour eigenstates

$$P(B \to \overline{B}) \neq P(\overline{B} \to B)$$

CP violation in decay

Unequal CP-conjugated decay rates

$$\Gamma(B \to f) \neq \Gamma(\overline{B} \to \overline{f})$$

CP violation in interference of decays with/without mixing

Time-dependent or time-integrated difference of decay rates of initial flavour eigenstates

$$\Gamma(B_{(\rightsquigarrow \overline{B})} \to f_{CP})(t) \neq \Gamma(\overline{B}_{(\rightsquigarrow B)} \to f_{CP})(t)$$

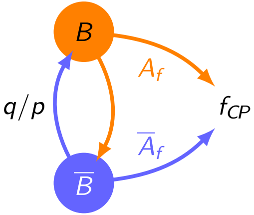

The Run 2 LHCb detector

LHCb detector performance
Int J Mod Phys A 30 (2015), 1530022

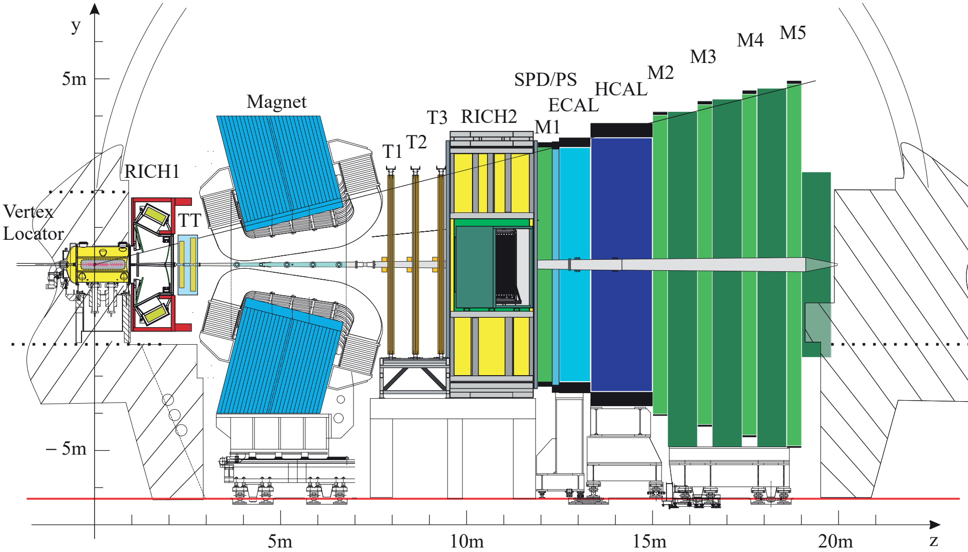

The Run 2 LHCb detector

LHCb detector performance
Int J Mod Phys A 30 (2015), 1530022

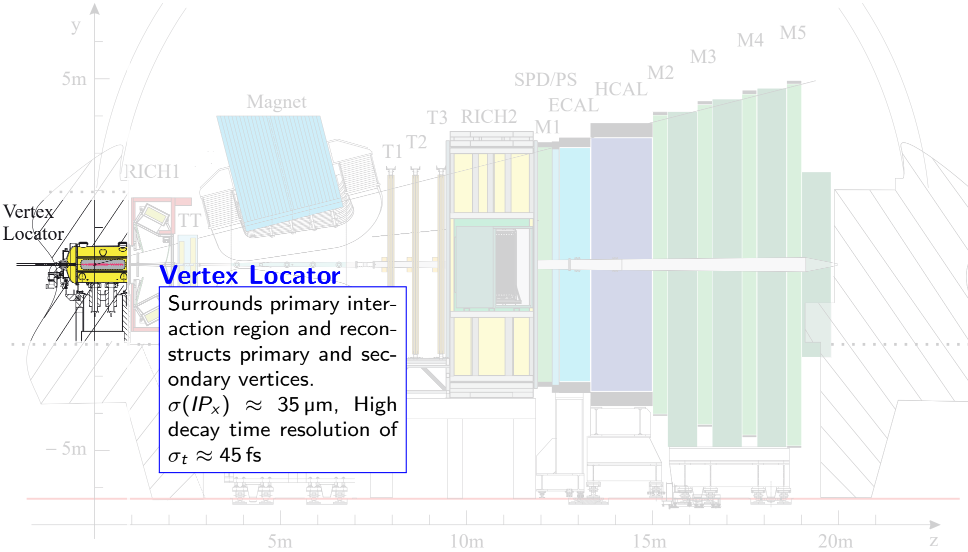

Vertex Locator

Surrounds primary interaction region and reconstructs primary and secondary vertices.
$\sigma(IP_x) \approx 35\,\mu m$, High decay time resolution of $\sigma_t \approx 45\,fs$

The Run 2 LHCb detector

LHCb detector performance
Int J Mod Phys A 30 (2015), 1530022

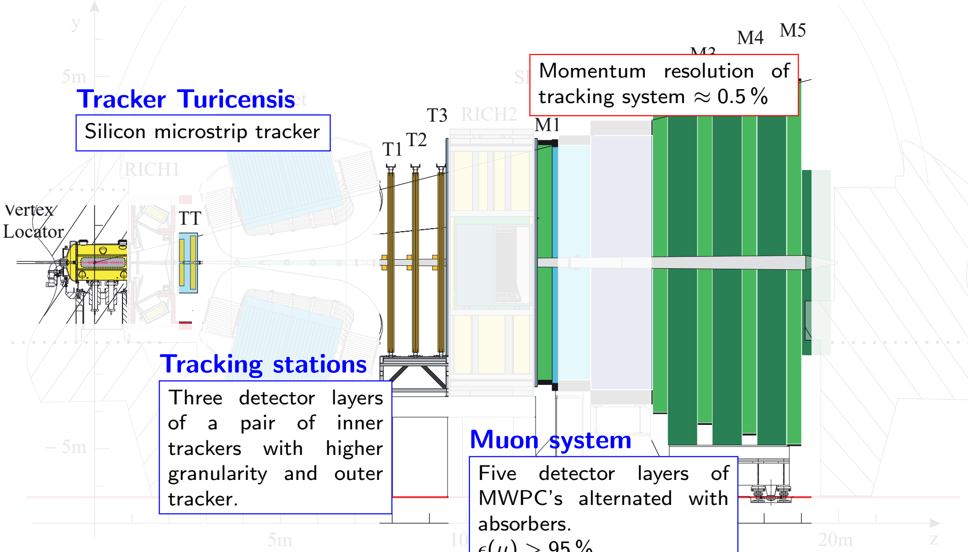

Tracker Turicensis

Silicon microstrip tracker

Tracking stations

Three detector layers of a pair of inner trackers with higher granularity and outer tracker.

Momentum resolution of tracking system $\approx 0.5\,\%$

Muon system

Five detector layers of MWPC's alternated with absorbers.
$\epsilon(\mu) > 95\,\%$

The Run 2 LHCb detector

LHCb detector performance
Int J Mod Phys A 30 (2015), 1530022

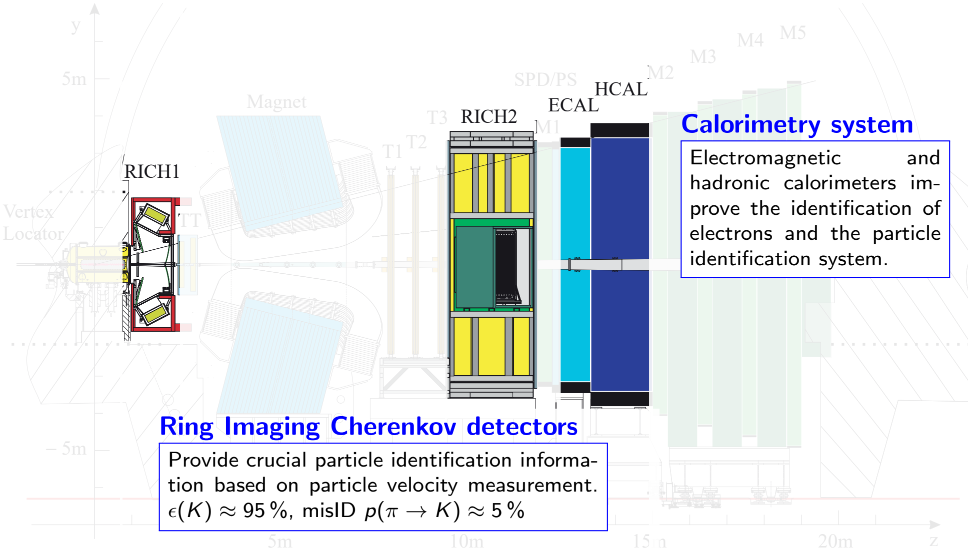

Calorimetry system

Electromagnetic and hadronic calorimeters improve the identification of electrons and the particle identification system.

Ring Imaging Cherenkov detectors

Provide crucial particle identification information based on particle velocity measurement. $\epsilon(K) \approx 95\,\%$, misID $p(\pi \to K) \approx 5\,\%$

Measurement of *CP* violation in $B^0 \to \psi K^0_\mathrm{S}$ decays

LHCb-Paper-2023-013 (In preparation)

Measurement of *CP* violation in $B^0 \to \psi K^0_S$ decays

The decay channel $B^0 \to \psi K^0_S$ offers a theoretically clean access to the CKM angle β.

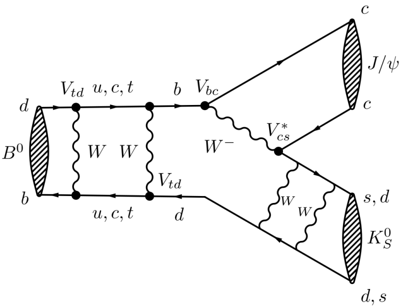

World average (HFLAV)

$$S = \quad 0.699 \pm 0.017$$
$$C = -0.005 \pm 0.015$$

$S = \sin(2\beta + \Delta\phi_d + \Delta\phi_d{}^{NP})$, penguin contributions are small: $\Delta\phi_d \approx 0.5\,\text{deg}$ [1]

$$\sin(2\beta) = \mathrm{Im}\left(\frac{q}{p}\frac{\overline{A}_{J/\psi K^0_S}}{A_{J/\psi K^0_S}}\right)$$

$$\beta = \arg\left(-\frac{V^*_{cb}V_{cd}}{V^*_{tb}V_{td}}\right)$$

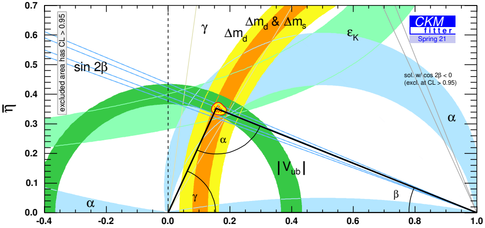

$\sin(2\beta) \neq 0 \Rightarrow$ *CP* violation

[1] J.Phys.G 48(2021) 065002

Measurement of CP violation in $B^0 \to \psi K^0_S$ decays

The decay channel $B^0 \to \psi K^0_S$ offers a theoretically clean access to the CKM angle β.

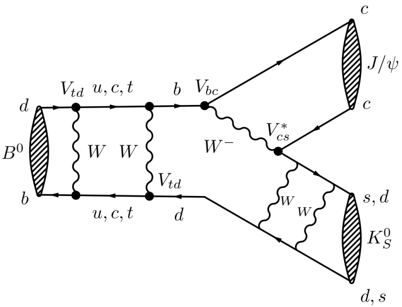

World average (HFLAV)

$$S = \quad 0.699 \pm 0.017$$
$$C = -0.005 \pm 0.015$$

$S = \sin(2\beta + \Delta\phi_d + \Delta\phi_d{}^{\mathrm{NP}})$, penguin contributions are small: $\Delta\phi_d \approx 0.5\,\mathrm{deg}$ [1]

$$\sin(2\beta) = \mathrm{Im}\left(\frac{q}{p}\frac{\overline{A}_{J/\psi\, K^0_S}}{A_{J/\psi\, K^0_S}}\right)$$

$$\beta = \arg\left(-\frac{V^*_{cb}V_{cd}}{V^*_{tb}V_{td}}\right)$$

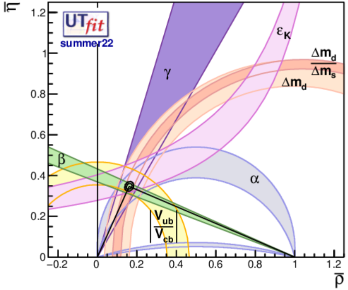

[1] J.Phys.G 48(2021) 065002

Measurement of CP violation in $B^0 \to \psi K^0_S$ decays

The decay channel $B^0 \to \psi K^0_S$ offers a theoretically clean access to the CKM angle β.

$$\mathcal{A}^{CP}(t) = \frac{\Gamma(\bar{B}^0(t) \to \psi K^0_S) - \Gamma(B^0(t) \to \psi K^0_S)}{\Gamma(\bar{B}^0(t) \to \psi K^0_S) + \Gamma(B^0(t) \to \psi K^0_S)} \approx \underbrace{D_{\Delta t} D_{FT}}_{\text{Experimental dilution factors}} \, S \sin(\Delta m_d t)$$

- We measure the three modes with the full Run 2 data set
  - $B^0 \to J/\psi(\to \mu\mu) K^0_S(\to \pi^+\pi^-)$ (82 %)
  - $B^0 \to J/\psi(\to ee) K^0_S(\to \pi^+\pi^-)$ (12 %)
  - $B^0 \to \psi(2S)(\to \mu\mu) K^0_S(\to \pi^+\pi^-)$ (6 %)
- Previous LHCb analyses:
  - [PRL 115 (2015) 031601]
  - [JHEP 11 (2017) 170]

Summary of most recent measurements

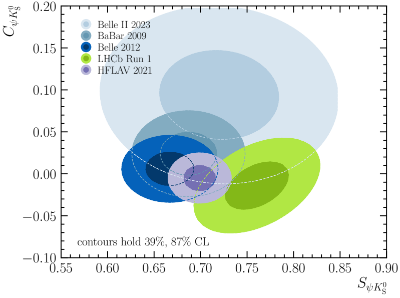

Candidate selection

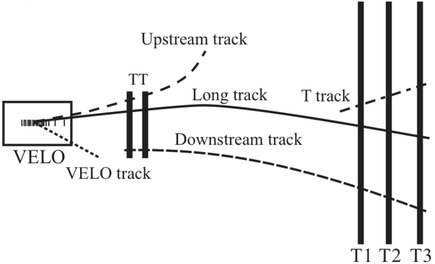

- Trigger
  - High p_{T} muon or electron pair with invariant mass near J/ψ or $\psi(2S)$ resonance
  - High p_{T} pion pair with good common vertex near K^0_{S} mass
- B^0 candidate vertex required to be separated from PV and be well reconstructed.
- Long K^0_{S} flight distance: In approx. 60 % of cases K^0_{S} leave VELO $\rightarrow$ use π candidates without VELO information

- For the first time in a LHCb *CPV* measurement
  - *upstream tracks* are considered, combined with *long track*
  - Combinations of long and *downstream tracks* are included
- New reco. categories add 13 % signal

Reduction of backgrounds

- Boosted decision tree to suppress combinatorial background
  - Signal proxy: Simulation
  - Background proxy: Upper mass side band
- $\Lambda_b^0 \to J/\psi\,\Lambda(\to p\pi^-)$: Require a low proton identification probability
- $B^0 \to J/\psi\,K^*(\to K^+\pi^-)$: Apply minimum K_S^0 decay time cut
- $B^+ \to J/\psi\,K^+(+\pi^-)$: Apply kaon mis-identification probability cut
- Remaining background from partially reconstructed B decays are modelled

Mass fits and signal yield

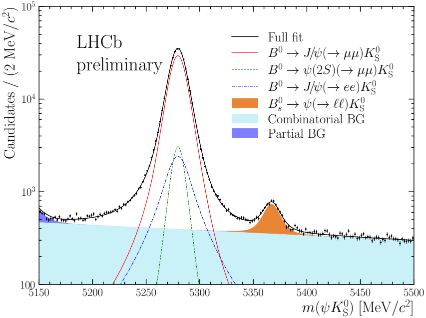

$$N_{J/\psi(\to\mu\mu)K^0_S} = 306\,322 \pm 619$$
$$N_{J/\psi(\to ee)K^0_S} = 42\,870 \pm 269$$
$$N_{\psi(2S)(\to\mu\mu)K^0_S} = 23\,570 \pm 164$$

From mass fits, *sWeights* are obtained for effective background subtraction in *CP* fit

- Signal modes: Double-sided Hypatia[1] distribution
- $B^0_s \to \psi K^0_S$: Shape shared with signal + constant shift
- Combinatorial background: Exponential distribution
- Partial background: Normal distribution

[1] Nucl. Instrum. Methods. Phys. Res. B 764 (2014) 150

Flavour Tagging at LHCb

The Flavour Tagging technique enables the identification of the B production flavour, allowing us to measure interference CP violation.

$$\mathcal{A}^{CP} = \frac{\Gamma(\overline{B}^0_{(s)} \to f_{CP}) - \Gamma(B^0_{(s)} \to f_{CP})}{\Gamma(\overline{B}^0_{(s)} \to f_{CP}) + \Gamma(B^0_{(s)} \to f_{CP})}$$

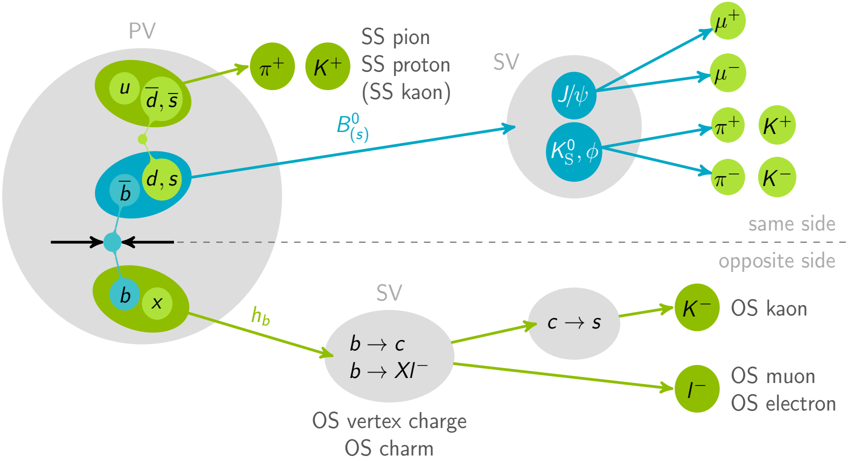

Flavour Tagging at LHCb

The Flavour Tagging technique enables the identification of the B production flavour, allowing us to measure interference CP violation.

$$\mathcal{A}^{CP} = \frac{\Gamma(\overline{B}^0_{(s)} \to f_{CP}) - \Gamma(B^0_{(s)} \to f_{CP})}{\Gamma(\overline{B}^0_{(s)} \to f_{CP}) + \Gamma(B^0_{(s)} \to f_{CP})}$$

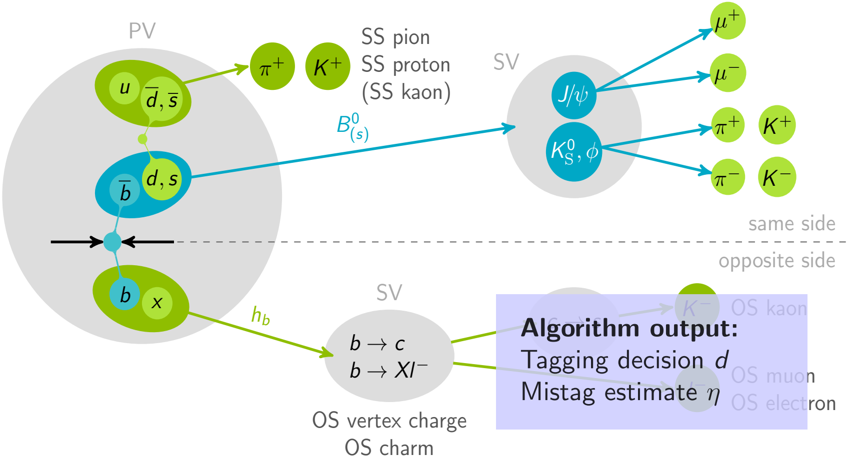

Algorithm output:
Tagging decision d
Mistag estimate η

Flavour Tagging approach

Control channel
$B^0 \to J/\psi K^{*0}$

Control channel
$B^+ \to J/\psi K^+$

Same Side Calibration

Opposite Side Calibration

Decay time fit $B^0 \to J/\psi K^*$

Use $J/\psi K^*$ starting parameters for SS

Constrain OS calibration to $J/\psi K^+$

Fit result

Calibration parameters

Production asymmetry

Flavour Tagging efficiency asymmetry

Full covariance matrix

Calibration procedure

Maximize tagging likelihood

$$\mathcal{L}(\vec{\theta}) = \prod_{j,\text{Wrong tag}}^{N} \omega(\eta_j, \vec{\theta}) \times \prod_{j,\text{Correct tag}}^{N} (1 - \omega(\eta_j, \vec{\theta}))$$

Tagging performance $\epsilon_{\text{tag}}(1-2\omega)^2$

$B^0 \to J/\psi(\to \mu\mu)K^0_S$: 4.02 %

$B^0 \to \psi(2S)(\to \mu\mu)K^0_S$: 3.92 %

$B^0 \to J/\psi(\to ee)K^0_S$: 5.98 %

CP fit model

Fit of time dependent B decay rates $P(B, t)$
Simplified model:

$$P_{CP}(t, d, \eta) \propto \left\{[1 + d(1 - 2\omega)]P_{B^0}(t) + [1 + d(1 - 2\overline{\omega})]P_{\bar{B}^0}(t)\right\}e^{-\Gamma t}$$

$$P_{B^0,(\bar{B}^0)}(t) \propto (1 \mp \alpha)(1 \mp \Delta\epsilon)(1 \mp \boldsymbol{S}\sin(\Delta m_d t) \pm \boldsymbol{C}\cos(\Delta m_d t))$$

CP fit model

Fit of time dependent B decay rates $P(B,t)$
Simplified model:

$$P_{CP}(t,d,\eta) \propto \left\{[1+d(1-2\omega)]P_{B^0}(t) + [1+d(1-2\overline{\omega})]P_{\overline{B}^0}(t)\right\} e^{-\Gamma t}$$

$$P_{B^0,(\bar{B}^0)}(t) \propto (1 \mp \alpha)(1 \mp \Delta\epsilon)(1 \mp S\sin(\Delta m_d t) \pm C\cos(\Delta m_d t))$$

- α Production asymmetry
- $\Delta\epsilon$ Flavour Tagging efficiency asymmetry
- S, C *CP*-violation parameters

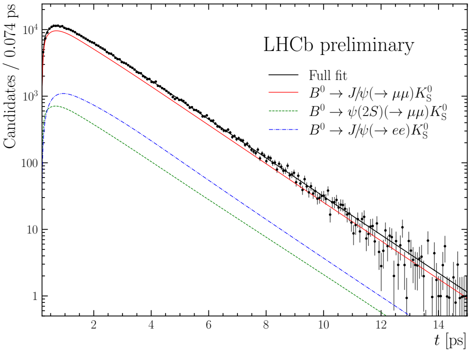

CP fit model

Fit of time dependent B decay rates $P(B, t)$
Simplified model:

$$P_{CP}(t, d, \eta) \propto \left\{[1 + d(1 - 2\omega)]P_{B^0}(t) + [1 + d(1 - 2\overline{\omega})]P_{\overline{B}^0}(t)\right\}e^{-\Gamma t}$$

$$P_{B^0,(\bar{B}^0)}(t) \propto (1 \mp \alpha)(1 \mp \Delta\epsilon)(1 \mp S \sin(\Delta m_d t) \pm C \cos(\Delta m_d t))$$

Decay time description

- Decay time acceptance model: Cubic splines
- Decay time resolution model: Optimized with simulation
- VELO misalignment calibrated with prompt data

Constrained parameters:
Δm_d, α, 8 FT calibration parameters via covariance matrix

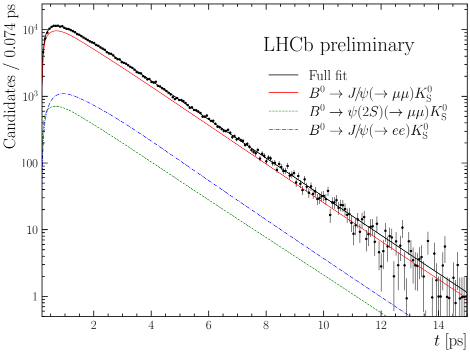

Systematic uncertainties

- **Fitter validation**
  - Generate toys of signal and background components
  - Fit toys, compare to generation values
- **$\Delta\Gamma_d$ uncertainty**
  - Vary $\Delta\Gamma_d$ by HFLAV uncertainty
- **FT calibration portability**
  - Compare transferred calibrations to MC truth calibration channels to calibrations on signal truth. Generate toys based on difference distribution.
- **FT $\Delta\epsilon$ portability**
  - Compare FT efficiency asymmetry on MC calibration channels and signal MC. Vary parameter in fit by difference
- **Decay-time bias model**
  - Decay time calibration parameters varied in 1σ bounds

Source	$\sigma(S)$	$\sigma(C)$
Fitter validation	0.0004	0.0006
$\Delta\Gamma_d$ uncertainty	0.0055	0.0017
FT calibration portability	0.0053	0.0001
FT $\Delta\epsilon_{\text{tag}}$ portability	0.0014	0.0017
Decay-time bias model	0.0007	0.0013

Analysis results

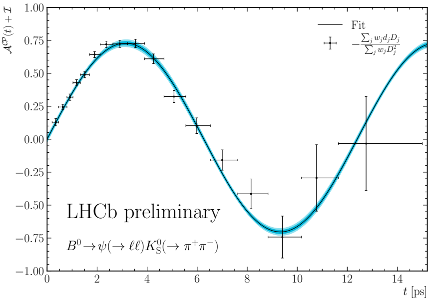

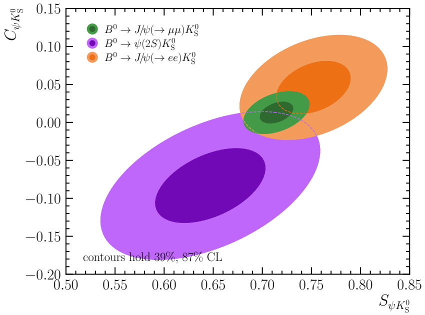

Combined fit result

$$S^{\text{Run 2}}_{\psi K^0_S} = 0.716 \pm 0.013\,(\text{stat}) \pm 0.008\,(\text{syst})$$
$$C^{\text{Run 2}}_{\psi K^0_S} = 0.012 \pm 0.012\,(\text{stat}) \pm 0.003\,(\text{syst})$$

Analysis results

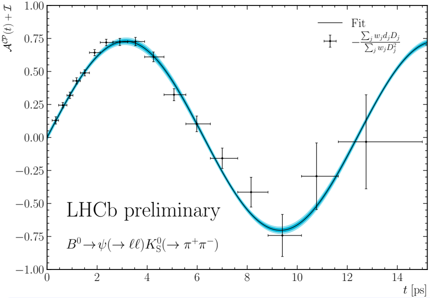

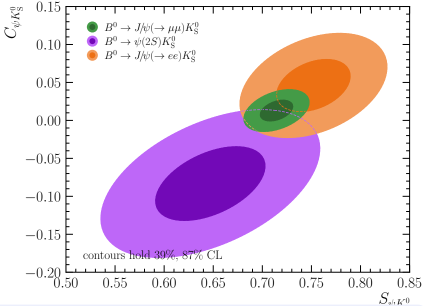

$$S^{\text{Run 2}}_{J/\psi(\to\mu^+\mu^-)K^0_S} = 0.714 \pm 0.015\,(\text{stat}) \pm 0.007\,(\text{syst})$$
$$C^{\text{Run 2}}_{J/\psi(\to\mu^+\mu^-)K^0_S} = 0.013 \pm 0.014\,(\text{stat}) \pm 0.003\,(\text{syst})$$
$$S^{\text{Run 2}}_{\psi(2S)K^0_S} = 0.647 \pm 0.053\,(\text{stat}) \pm 0.018\,(\text{syst})$$
$$C^{\text{Run 2}}_{\psi(2S)K^0_S} = -0.083 \pm 0.048\,(\text{stat}) \pm 0.005\,(\text{syst})$$
$$S^{\text{Run 2}}_{J/\psi(\to e^+e^-)K^0_S} = 0.752 \pm 0.037\,(\text{stat}) \pm 0.084\,(\text{syst})$$
$$C^{\text{Run 2}}_{J/\psi(\to e^+e^-)K^0_S} = 0.046 \pm 0.034\,(\text{stat}) \pm 0.008\,(\text{syst})$$

Combination of LHCb (S, C) measurements

Combination strategy

- Combinations of Run 1 and Run 2 single measurements are performed
- Input parameter systematics Δm_d, $\Delta\Gamma_d$, α assumed to be correlated

New total LHCb combination

$$S_{\psi K^0_S}^{\text{Run 1+2}} = 0.723 \pm 0.014\,(\text{stat+syst})$$
$$C_{\psi K^0_S}^{\text{Run 1+2}} = 0.007 \pm 0.012\,(\text{stat+syst})$$

Combination of $B^0 \to J/\psi\, K^0_S$ modes

$$S_{J/\psi K^0_S}^{\text{Run 1+2}} = 0.724 \pm 0.014\,(\text{stat+syst})$$
$$C_{J/\psi K^0_S}^{\text{Run 1+2}} = 0.013 \pm 0.012\,(\text{stat+syst})$$

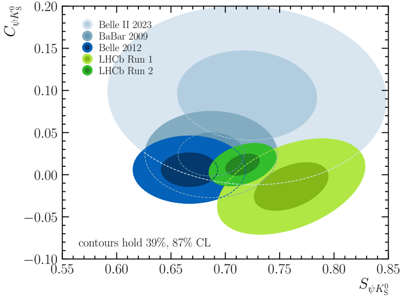

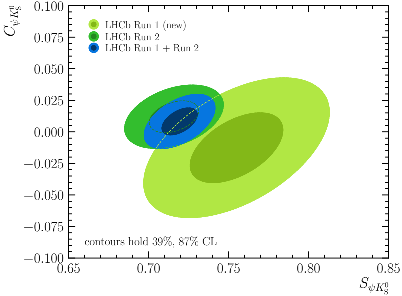

Summary and preliminary HFLAV 2023 combinations

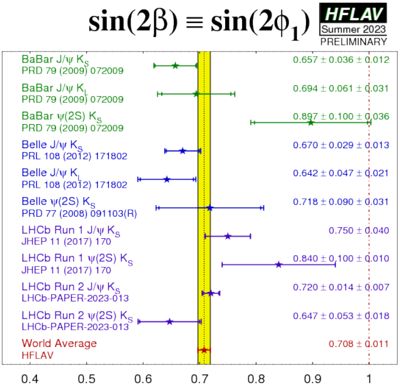

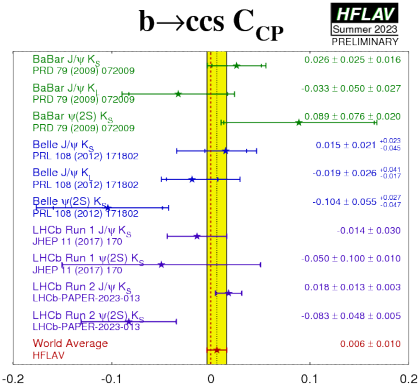

- **This measurement is the most precise single measurement of sin(2β) to date**
- **The statistical uncertainty is still the limiting factor**

Summary and preliminary HFLAV 2023 combinations

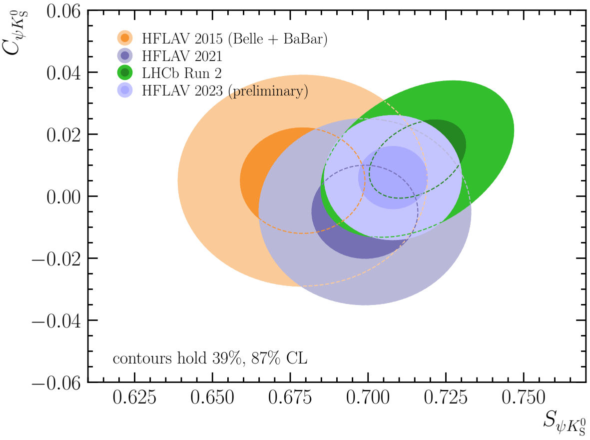

- **This measurement is the most precise single measurement of $\sin(2\beta)$ to date**
- **The statistical uncertainty is still the limiting factor**

Measurement of CP violation in $B_s^0 \to J/\psi K^+K^-$

LHCb-Paper-2023-016 (In preparation)

$B_s^0 - \overline{B}_s^0$ oscillations

- Oscillation much faster than B^0 ($\Delta m_s \gg \Delta m$)
  - Precise determination of time resolution is crucial
- Non-zero $\Delta\Gamma_s$

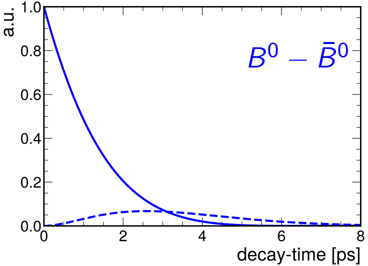

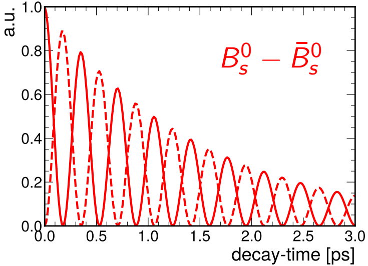

oscillation
$\Delta m \sim 0.5\ \text{ps}^{-1}$
$\tau(B^0) \sim 1.52$ ps

very fast oscillation
$\Delta m_s \sim 17.765\ \text{ps}^{-1}$
$\tau(B_s^0) \sim 1.52$ ps

$B_s^0 - \overline{B}_s^0$ oscillations

- Most precise measurement at LHCb

  $\Delta m_s = (17.7656 \pm 0.0057)\,\text{ps}^{-1}$ Nat. Phys. 18(2022)1-5

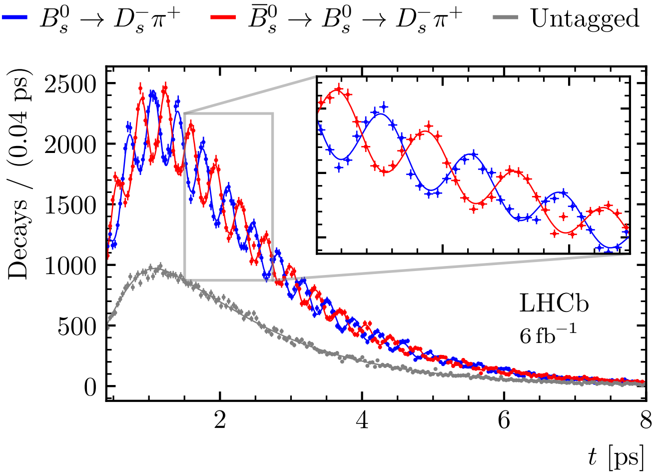

CP violation in B_s^0 mixing and decays

- Mixing-induced CPV phase ϕ_s in B_s^0 decays through $b \to c\bar{c}s$ transitions
  - highly suppressed compared to the B^0 system ($\beta \sim 22^\circ \approx 0.39$ rad)
  - CKM global fit: $\phi_s^{\text{tree}} \approx -2\beta_s = (-0.0368^{+0.0006}_{-0.0009})$ rad[1]
  - UT fitter: $-2\beta_s = -0.0370 \pm 0.0010$ rad

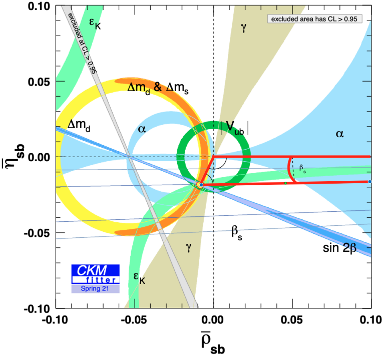

$$V_{us}V_{ub}^* + V_{cs}V_{cb}^* + V_{ts}V_{tb}^* = 0$$

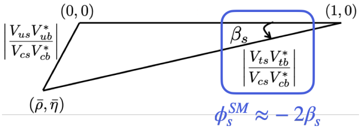

[1] Ignoring penguin contribution

CP violation in B_s^0 mixing and decays

- Sensitive to physics beyond the SM, up to $>$ TeV scale
  - can enter in internal loops Rev.Mod.Phys. 88(2016)045002
  - can lead to sizable modification to ϕ_s

$$\phi_s = \phi_s^{\rm tree} + \delta\phi_s^{\rm penguin} + \delta\phi_s^{NP}$$

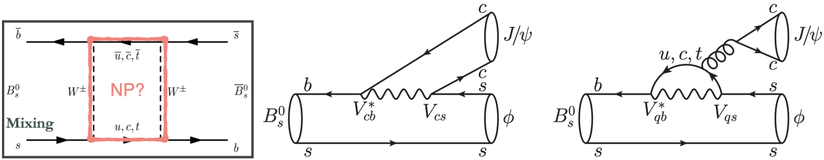

- Golden channel: $B_s^0 \to J/\psi\phi$
  - A small fraction of S-wave component $\to$ making it possible to determine the sign of $\Delta\Gamma_s$ LHCB-PAPER-2011-028
  - Measurements of Γ_s, $\Delta\Gamma_s$, Δm_s, strong phases & polarisation fractions

Experimental measurements

- First results from CDF and D0 with big uncertainties
- Combined result from CDF, D0, ATLAS, CMS & LHCb:

$$\Delta\Gamma_s = (0.082 \pm 0.005)\ \mathrm{ps}^{-1} \qquad \text{[HFLAV]}$$

$$\phi_s^{J/\psi KK} = 0.070 \pm 0.022\ \mathrm{rad}, \quad \phi_s^{c\bar{c}s} = -0.049 \pm 0.019\ \mathrm{rad}$$

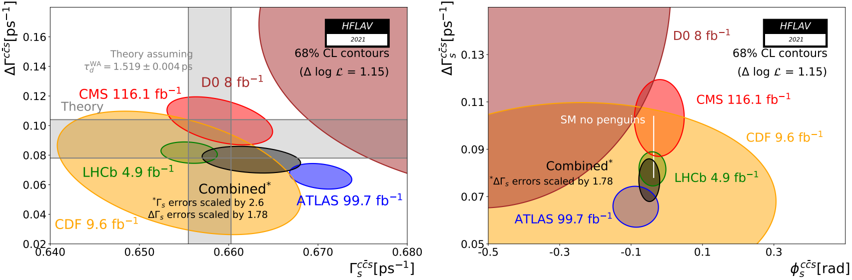

- Including measurements from $B_s^0 \to J/\psi\pi^+\pi^-$, $B_s^0 \to J/\psi(e^+e^-)K^+K^-$, $B_s^0 \to \psi K^+K^-$, $B_s^0 \to D_s^+D_s^-$, etc by LHCb

Measuring ϕ_s

$$A_{CP}(t) = \frac{\Gamma(\bar{B}_s^0 \to J/\psi KK) - \Gamma(B_s^0 \to J/\psi KK)}{\Gamma(\bar{B}_s^0 \to J/\psi KK) + \Gamma(B_s^0 \to J/\psi KK)} = \eta_f \cdot \sin \phi_s^{\mathrm{obs}} \cdot \sin(\Delta m_s t)$$

- CP eigenvalue of the final state $\eta_f = (-1)^L$

Measuring ϕ_s

$$A_{CP}(t) = \frac{\Gamma(\bar{B}_s^0 \to J/\psi KK) - \Gamma(B_s^0 \to J/\psi KK)}{\Gamma(\bar{B}_s^0 \to J/\psi KK) + \Gamma(B_s^0 \to J/\psi KK)} = \eta_f \cdot \sin \phi_s^{\mathrm{obs}} \cdot \sin(\Delta m_s t)$$

- *CP* eigenvalue of the final state $\eta_f = (-1)^L$
- A mixture of *CP*-even & *CP*-odd components $\to$ angular analysis

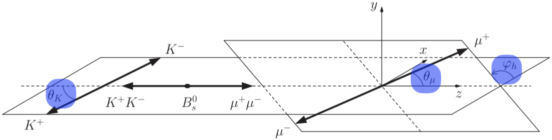

Measuring ϕ_s

$$A_{CP}(t) = \frac{\Gamma(\bar{B}_s^0 \to J/\psi KK) - \Gamma(B_s^0 \to J/\psi KK)}{\Gamma(\bar{B}_s^0 \to J/\psi KK) + \Gamma(B_s^0 \to J/\psi KK)} = \eta_f \cdot \sin\phi_s^{\mathrm{obs}} \cdot \sin(\Delta m_s t)$$

- *CP* eigenvalue of the final state $\eta_f = (-1)^L$
- A mixture of *CP*-even & *CP*-odd components $\to$ angular analysis

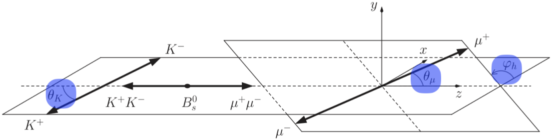

Experimentally:

$$A_{CP}(t) \propto \eta_f \cdot e^{-\frac{1}{2}\Delta m_s^2 \sigma_t^2} \cdot (1 - 2\omega) \cdot \sin\phi_s^{\mathrm{obs}} \cdot \sin(\Delta m_s t)$$

- Probability of mis-tagging the B_s^0 flavor at production, ω
- Excellent decay-time resolution $\sigma_t \sim 42$ fs
- Model for decay-time and angular efficiencies

Candidates selection

Clean signatures of signals: $B_s^0 \to J/\psi K^+K^-$ around $\phi(1020)$ vicinity

- Hardware trigger (L0) depends on high p_T from Calo/Muon detector
- Full event reconstruction in software trigger stages
  - *time unbiased*: $m(\mu^+\mu^-) > 2.7\ \mathrm{GeV}/c^2$
  - *time biased*: significant displacement from PV or a good-quality di-muon secondary vertex
- Boosted Decision Tree to suppress combinatorial background

Candidates selection

Clean signatures of signals: $B_s^0 \to J/\psi K^+ K^-$ around $\phi(1020)$ vicinity

- Hardware trigger (L0) depends on high p_T from Calo/Muon detector
- Full event reconstruction in software trigger stages
  - *time unbiased*: $m(\mu^+\mu^-) > 2.7\ \mathrm{GeV}/c^2$
  - *time biased*: significant displacement from PV or a good-quality di-muon secondary vertex
- Boosted Decision Tree to suppress combinatorial background

- Tight particle identification and mass requirements to veto peaking backgrounds
  - $B^0 \to J/\psi K^+ \pi^-$ negligible after veto
  - $\Lambda_b^0 \to J/\psi p K^-$ is subtracted with negative weights from simulation

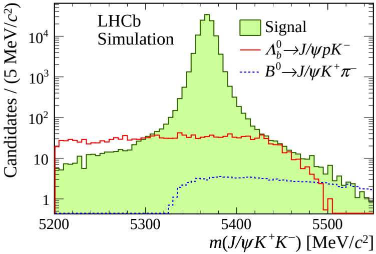

EPJC79(2019)706

Mass fit

- Splot technique to subtract backgrounds
  - Double-sided Crystall-ball for signal, with width parametrised as a function of σ_m to reduce correlation with $\cos\theta_\mu$
  - $B^0 \to J/\psi K^+K^-$ shares signal shape except for the mean of mass
  - Exponential function for combinatorial background
  - Separate fits in six $m(K^+K^-)$ bins, two trigger categories and 4 years (15-18)

$\rightarrow$ Signal candidates: 349000

$\phi(1020)$ + small S-waves

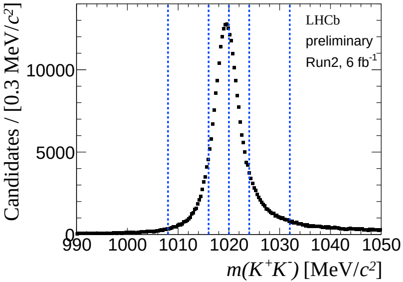

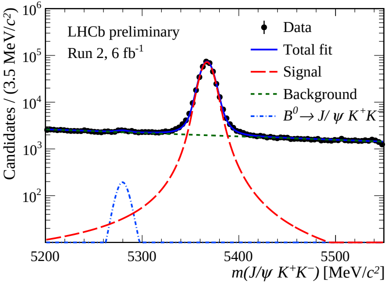

Flavour tagging calibration

OS tagging

- Calibration channel: $B^+ \to J/\psi K^+$
- Counting correct/mis-tagged events according to K charge

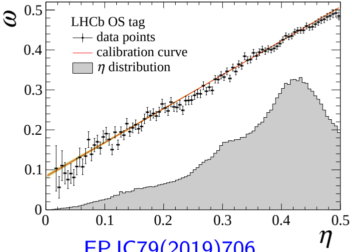

EPJC79(2019)706

SSK tagging

- Calibration channel: $B_s^0 \to D_s^- \pi^+$
- Fit to the time distribution in 8 bins of the predicted mistag probability η

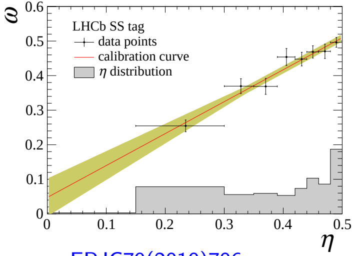

EPJC79(2019)706

Flavour tagging calibration

OS tagging

- Calibration channel: $B^+ \to J/\psi K^+$
- Counting correct/mis-tagged events according to K charge

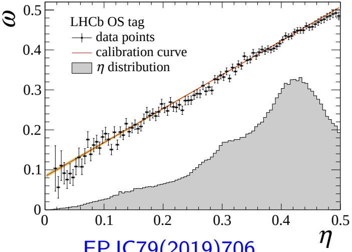

EPJC79(2019)706

SSK tagging

- Calibration channel: $B_s^0 \to D_s^- \pi^+$
- Fit to the time distribution in 8 bins of the predicted mistag probability η

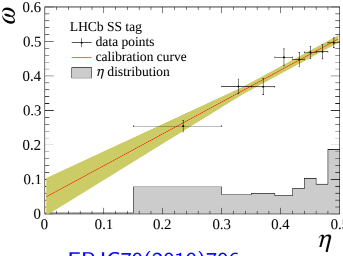

EPJC79(2019)706

- Linear calibration: $\omega = p_0 + p_1(\eta - \langle\eta\rangle)$
- Tagging power of combined OS and SSK taggers

year	2015+2016	2017	2018
$\epsilon_{\rm tag}(1-\omega)^2$	$(4.18 \pm 0.15)\%$	$(4.22 \pm 0.16)\%$	$(4.36 \pm 0.16)\%$

Decay-time resolution

$\mathcal{G}(t-\mu|\sigma_{\text{eff}})$

- Decay time resolution dilutes oscillations, $\mathcal{D} = exp(-\frac{1}{2}\sigma^2_{\text{eff}}\Delta m_s^2)$

$$\delta_t^2 \approx (\frac{m}{p})^2\sigma_L^2 + (\frac{t}{p})^2\sigma_p^2$$

$$\sigma_L \sim 200\,\mu\text{m}, \sigma_p/p \sim 0.5\%$$

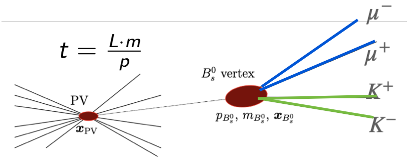

Decay-time resolution

$\mathcal{G}(t-\mu|\sigma_{\rm eff})$

- Decay time resolution dilutes oscillations, $\mathcal{D} = exp(-\frac{1}{2}\sigma_{\rm eff}^2 \Delta m_s^2)$

$$\delta_t^2 \approx (\frac{m}{p})^2 \sigma_L^2 + (\frac{t}{p})^2 \sigma_p^2$$

$$\sigma_L \sim 200\,\mu\text{m}, \sigma_p/p \sim 0.5\%$$

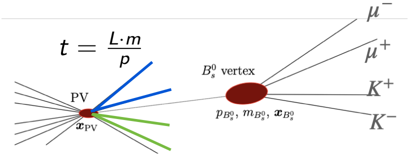

- Prompt $J/\psi KK$ events with all tracks coming from pp collision (PV)
  - $t = 0 \pm \sigma_t$, where σ_t reflects resolution effect of the detector
- Effective Gaussian resolution, with width parameterised as $\sigma_{\rm eff} = p_0 + p_1\delta_t \to$ 42 fs in average, $\mathcal{D} \sim 0.75$
- Small bias (~ 5 fs) due to tiny misalignment in VELO is corrected by adding as mean μ of the Gaussian resolution model

Decay-time efficiency

- Reconstruction and selection introduce non-uniform efficiency
- Data-driven method using control channel $B^0 \to J/\psi K^{*0}(\to K^+\pi^-)$
  - $\tau_{B^0} = (1.520 \pm 0.004)$ ps, $\Delta\Gamma_d = 0\ \mathrm{ps}^{-1}$
  - B_s^0 ($\Delta\Gamma_s = 0$) and B^0 simulations to account for kinematic difference between signal and control mode

$$\varepsilon^{B_s^0}_{\mathrm{data}}(t) = \varepsilon^{B^0}_{\mathrm{data}}(t) \times \frac{\varepsilon^{B_s^0}_{\mathrm{sim}}(t)}{\varepsilon^{B^0}_{\mathrm{sim}}(t)}$$

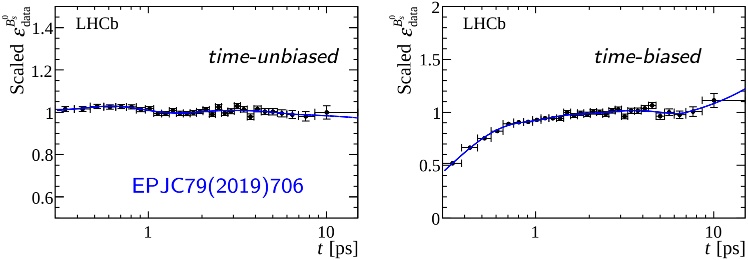

✔ Validated by measuring the lifetime of B^0 and B^+ using $B^0 \to J/\psi K^{*0}$ and $B^+ \to J/\psi K^+$ data

Angular efficiencies

- Detector geometry and selection criteria introduce non-uniform efficiency
- Estimated with $B_s^0 \to J/\psi\phi$ simulation
- Iterative procedure to correct the difference between simulation and data

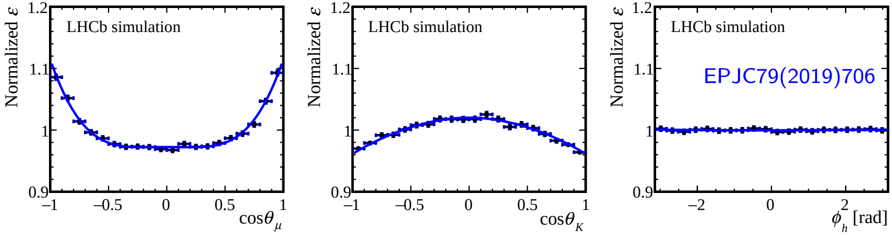

✔ Validated by measuring the polarisation amplitudes of $B^0 \to J/\psi K^{*0}$

Fit results

- Simultaneous fit to 48 sub-samples: 4 years $\times$ 2 trigger categories $\times$ 6 $m(KK)$
- Tagging calibration parameters and spline coefficiencies of time acceptance are Gaussian constraint
- Extract physics parameters: ϕ_s, λ, $\Delta\Gamma_s, \Gamma_s - \Gamma_d$, Δm_s

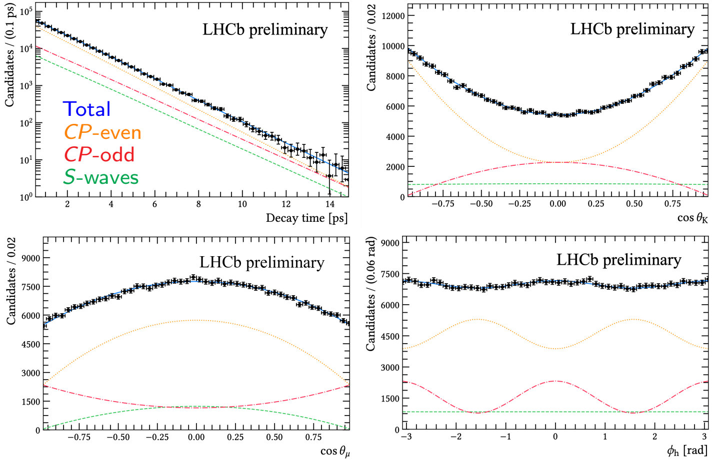

Systematic uncertainties

* Uncertainties ($\times 0.01$) Dominant sys. Sub-dominant sys. Stat. limited

Source	$\lvert A_0\rvert^2$	$\lvert A_\perp\rvert^2$	ϕ_s [rad]	$\lvert\lambda\rvert$	$\delta_\perp - \delta_0$ [rad]	$\delta_\parallel - \delta_0$ [rad]	$\Gamma_s - \Gamma_d$ [ps^{-1}]	$\Delta\Gamma_s$ [ps^{-1}]	Δm_s [ps^{-1}]
Mass parametrization	0.04	0.03	0.03	0.02	0.15	0.12	0.02	0.04	0.03
Mass: shape statistical	0.04	0.04	0.05	0.09	0.62	0.33	0.02	0.01	0.11
Mass factorization	0.11	0.10	0.42	0.19	0.54	0.60	0.12	0.16	0.18
B_c^+ contamination *	0.04	0.05	—	0.02	—	0.17	(0.07)	(0.03)	—
D–wave component	0.04	0.04	0.02	—	0.07	0.13	0.01	0.03	0.02
Ghost tracks	0.07	0.04	0.02	0.10	0.18	0.18	0.02	—	0.01
Multiple candidates	0.01	—	0.27	0.22	0.90	0.41	0.01	0.01	0.24
Particle identification	0.06	0.09	0.27	0.27	1.31	0.51	0.05	0.15	0.46
$C_{\rm SP}$ factors	—	0.01	0.01	0.03	0.73	0.41	—	0.01	0.04
DTR model portability	—	—	0.08	0.03	0.26	0.09	—	—	0.09
DTR calibration	—	—	0.03	0.02	0.11	0.07	—	—	0.05
Time bias correction	0.04	0.05	0.06	0.05	0.77	0.11	0.03	0.05	0.44
Angular efficiency	0.05	0.14	0.25	0.32	0.42	0.44	0.01	0.02	0.13
Angular resolution	0.01	0.01	0.02	0.01	0.02	0.08	—	0.01	0.02
Kinematic weighting	0.24	0.09	0.01	0.01	0.98	0.86	0.02	0.03	0.31
Momentum uncertainty	0.08	0.04	0.04	—	0.07	0.11	0.01	—	0.13
Longitudinal scale	0.07	0.04	0.04	—	0.10	0.09	0.02	—	0.31
Neglected correlations	—	—	—	—	4.20	4.96	—	—	—
Total sys. unc.	0.32	0.24	0.6	0.5	4.8	5.2	0.14	0.24	0.9
Stat. unc.	0.17	0.23	2.2	1.1	7.5	6.0	0.14	0.44	3.3

*The uncertainty of the B_c^+ contamination for $\Delta\Gamma_d^s$ and $\Delta\Gamma_s$ is included in the fit to data and does not contribute to the quoted total systematic uncertainty.

Results

Parameters	Values [2]
ϕ_s [rad]	$-0.039 \pm 0.022 \pm 0.006$
$\|\lambda\|$	$1.001 \pm 0.011 \pm 0.005$
$\Gamma_s - \Gamma_d$ [ps^{-1}]	$-0.0056 ^{+0.0013}_{-0.0015} \pm 0.0014$
$\Delta\Gamma_s$ [ps^{-1}]	$0.0845 \pm 0.0044 \pm 0.0024$
Δm_s [ps^{-1}]	$17.743 \pm 0.033 \pm 0.009$
$\|A_\perp\|^2$	$0.2463 \pm 0.0023 \pm 0.0024$
$\|A_0\|^2$	$0.5179 \pm 0.0017 \pm 0.0032$
$\delta_\perp - \delta_0$ [rad]	$2.903 ^{+0.075}_{-0.074} \pm 0.048$
$\delta_\parallel - \delta_0$ [rad]	$3.146 \pm 0.060 \pm 0.052$

Run 1 result: $\phi_s = -0.058 \pm 0.049 \pm 0.006$ rad

- The most precise measurement of ϕ_s to date
- Compatible with the prediction from SM Global fits
- No evidence for *CP* violation

[2] The first uncertainty is statistical and the second systematic.

Polarisation-dependent fit

New physics effects can vary in different polarisation states

- Allow $|\lambda|$ and ϕ_s differ in polarisation states
- Shows no evidence for any polarisation dependence

Parameters	Values (stat. unc. only)
ϕ_s^0 [rad]	-0.034 ± 0.023
${\phi_s}^{\parallel} - \phi_s^0$ [rad]	-0.002 ± 0.021
${\phi_s}^{\perp} - \phi_s^0$ [rad]	$-0.001\,^{+0.020}_{-0.021}$
${\phi_s}^{S} - \phi_s^0$ [rad]	$0.022\,^{+0.027}_{-0.026}$
$\lvert\lambda^0\rvert$	$0.969\,^{+0.025}_{-0.024}$
$\lvert\lambda^{\parallel}/\lambda^0\rvert$	$0.982\,^{+0.055}_{-0.052}$
$\lvert\lambda^{\perp}/\lambda^0\rvert$	$1.107\,^{+0.082}_{-0.076}$
$\lvert\lambda^{S}/\lambda^0\rvert$	$1.121\,^{+0.084}_{-0.078}$

Combination with all measurements

- $\phi_s^{J/\psi KK} = -0.050 \pm 0.017$ rad $\rightarrow$ improved by 23%
- $\phi_s^{c\bar{c}s} = -0.039 \pm 0.016$ rad $\rightarrow$ improved by 15%
- Consistent with the prediction of Global fits assuming SM:[3]

$$\phi_s^{\mathrm{CKMfitter}} \approx (-0.0368^{+0.0006}_{-0.0009})\ \mathrm{rad},\ \phi_s^{\mathrm{UTfitter}} = -0.0370 \pm 0.0010\ \mathrm{rad}$$

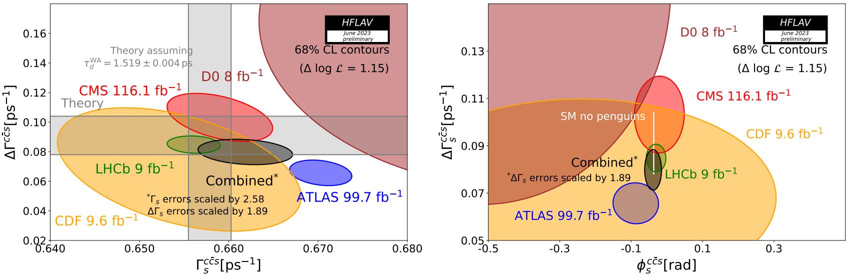

[3] Ignoring penguin contribution.

ϕ_s in $b \to s\bar{s}s$ transition

LHCb-Paper-2023-001

- Penguin dominated decay $B_s^0 \to \phi(\to K^+K^-)\phi(\to K^+K^-)$
- NP contributes to mixing and penguin processes

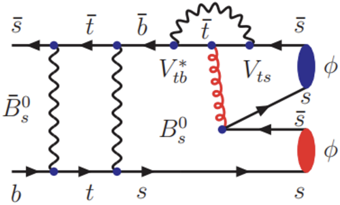

ϕ_s in $b \to s\bar{s}s$ transition

LHCb-Paper-2023-001

- Penguin dominated decay $B_s^0 \to \phi(\to K^+K^-)\phi(\to K^+K^-)$
- NP contributes to mixing and penguin processes

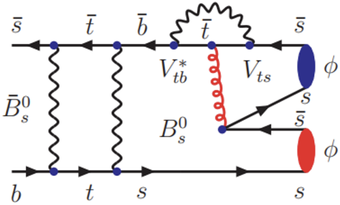

- Very similar analysis strategy as $B_s^0 \to J/\psi K^+K^-$
  $\to$ Flavor-tagged time-dependent angular analysis

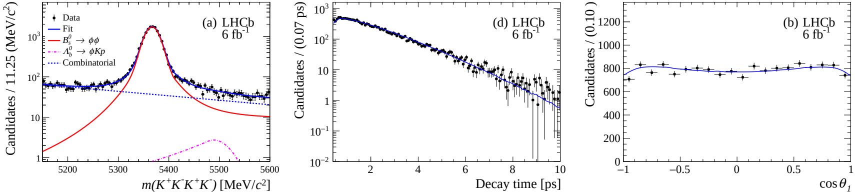

ϕ_s in $b \to s\bar{s}s$ transition

LHCb-Paper-2023-001

$$\phi_s^{s\bar{s}s} = -0.042 \pm 0.075 \pm 0.009 \text{ rad}$$
$$|\lambda| = 1.004 \pm \pm 0.030 \pm 0.009$$

- The most precise mesurement of $\phi_s^{s\bar{s}s}$ in penguin dominated decays
- No *CP* violation is observed

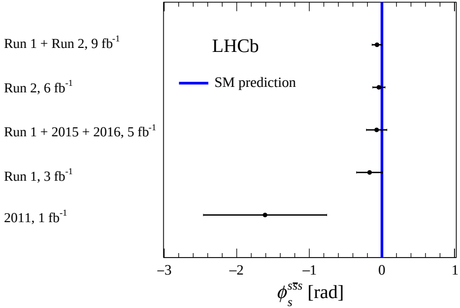

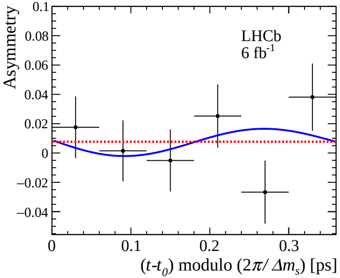

Looking at Run 3 and beyond

Looking at Run 3 and beyond

- Further precision improvement with more data

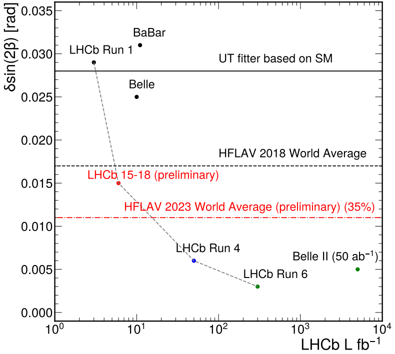

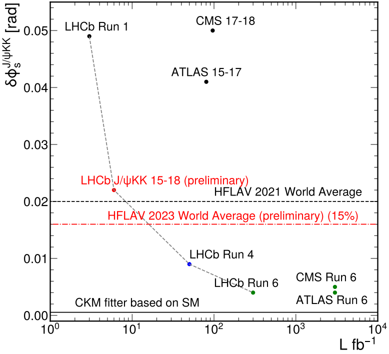

LHCb-PUB-2018-009, PoS(KMI2017)005, ATL-PHYS-PUB-2018-041, CMS-PAS-FTR-18-041

Looking at Run 3 and beyond

- Further precision improvement with more data

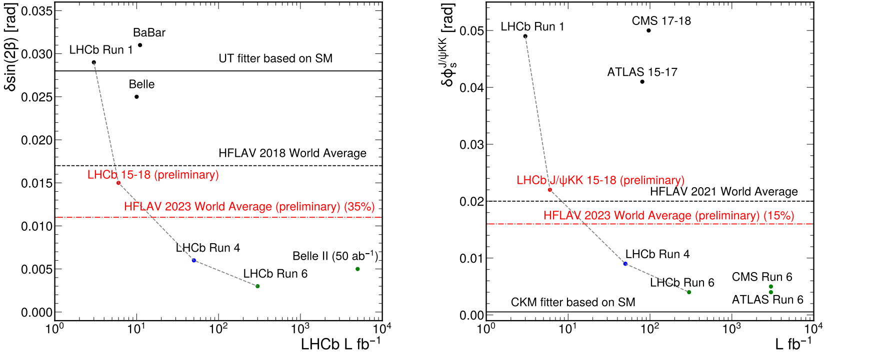

LHCb-PUB-2018-009, PoS(KMI2017)005, ATL-PHYS-PUB-2018-041, CMS-PAS-FTR-18-041

- Great opportunities to search for NP indirectly, up to > TeV scale

Controlling the penguin effects

- $\sigma(\phi_s) \sim 0.016$ comparable with the estimation of $\Delta\phi_s^{penguin} \sim 1^\circ \approx 0.017$
  $\rightarrow$ Better control of penguin effect necessary!
- Combined analysis of penguin contributions in ϕ_s and ϕ_d, using SU(3) flavor symmetry J.Phys.G 48 (2021) 6, 065002
- More experimental measurements come soon!

$$\phi_d = \sin(2\beta^{\text{tree}}) + \Delta\phi_d{}^{\text{penguin}} + \phi_d{}^{\text{NP}}$$
$$\phi_s = \phi_s^{\text{tree}} + \Delta\phi_s^{\text{penguin}} + \phi_s^{NP}$$

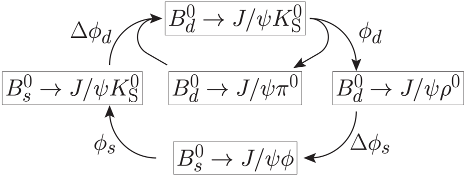

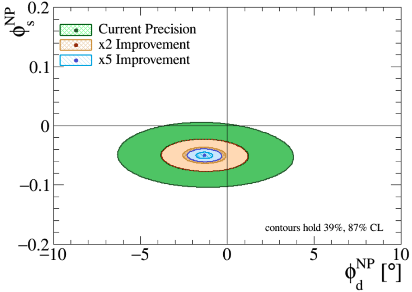

Summary

- Flag-ship time-dependent measurements of *CP* violation with the full LHCb Run 1 & 2 data sample, giving the most precise measurements:
  - $\sin 2\beta$ with $B^0 \to \psi K^0_S$
    $\sin(2\beta) = 0.716 \pm 0.013 \pm 0.008 \to$ improving WA by 35%
  - ϕ_s with $B^0_s \to J/\psi K^+ K^-$
    $\phi_s = -0.039 \pm 0.022 \pm 0.006 \text{ rad} \to$ improving WA by 15%
  - $\phi_s^{s\bar{s}s}$ in penguin dominated decays
    $\phi_s^{s\bar{s}s} = -0.042 \pm 0.075 \pm 0.009 \text{ rad}$
- Still statistics limited, Upgrade I and II needed to further test the SM and search for NP indirectly

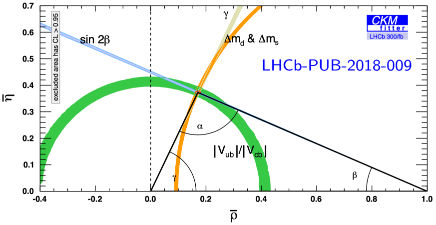

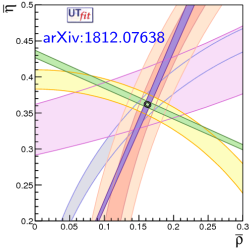

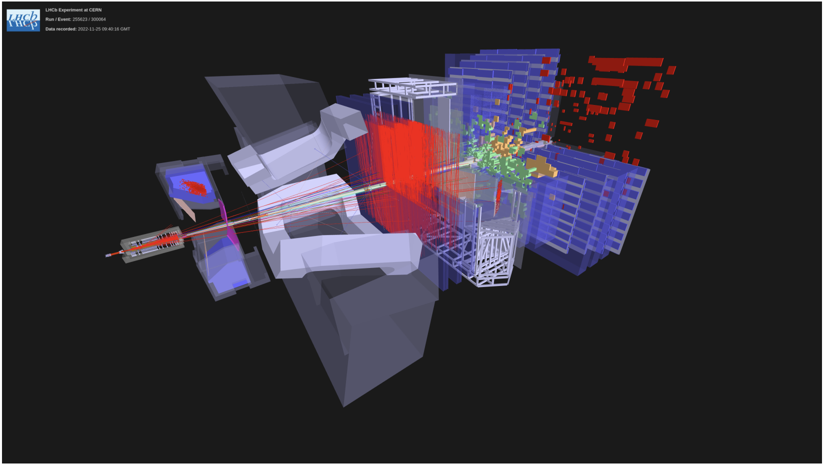

Thank you for your attention!

PDF for ϕ_s

Time-dependent angular fit

EPJC79(2019)706

$$\mathscr{P}(t, \theta_K, \theta_\mu, \phi_h | \delta_t) \propto \sum_{k=1}^{10} N_k h_k(t) f_k(\theta_K, \theta_\mu, \phi_h) \rightarrow \phi_s,\ \Delta m_s,\ \Delta\Gamma_s,\ \Gamma_s - \Gamma_d$$

$$\mathcal{P}\left(t, \Omega | \mathrm{q}^{\mathrm{OS}}, \mathrm{q}^{\mathrm{SSK}}, \eta^{\mathrm{OS}}, \eta^{\mathrm{SSK}}, \delta_t\right)$$
$$\propto \sum_{k=1}^{10} C_{\mathrm{SP}}^k N_k f_k(\Omega) \varepsilon_{\mathrm{data}}^{B_s^0}(t)$$
$$\cdot \left\{\left[\mathcal{Q}\left(\mathrm{q}^{\mathrm{OS}}, \mathrm{q}^{\mathrm{SSK}}, \eta^{\mathrm{OS}}, \eta^{\mathrm{SSK}}\right) h_k\left(t | B_s^0\right) + \bar{\mathcal{Q}}\left(\mathrm{q}^{\mathrm{OS}}, \mathrm{q}^{\mathrm{SSK}}, \eta^{\mathrm{OS}}, \eta^{\mathrm{SSK}}\right) h_k\left(t | \bar{B}_s^0\right)\right] \otimes \mathcal{R}\left(t - t' | \delta_t\right)\right\}$$

Angular amplitudes

C_{SP}^k account for the interference between P- and S- wave

flavor tagging

time-dependent oscillation

decay-time efficiency

decay-time resolution

$$h_k(t|B_s^0) = \frac{3}{4\pi} e^{-\Gamma t}\left(a_k \cosh\frac{\Delta\Gamma t}{2} + b_k \sinh\frac{\Delta\Gamma t}{2} + c_k \cos(\Delta m t) + d_k \sin(\Delta m t)\right),$$

$$h_k(t|\bar{B}_s^0) = \frac{3}{4\pi} e^{-\Gamma t}\left(a_k \cosh\frac{\Delta\Gamma t}{2} + b_k \sinh\frac{\Delta\Gamma t}{2} - c_k \cos(\Delta m t) - d_k \sin(\Delta m t)\right),$$

a_k, b_k, c_k, d_k involve strong and weak phases (δ, ϕ_s) of each component

k	A_k	$f_k(\theta_\mu, \theta_K, \varphi_h)$
1	$\lvert A_0\rvert^2$	$2\cos^2\theta_K \sin^2\theta_\mu$
2	$\lvert A_\parallel\rvert^2$	$\sin^2\theta_k(1 - \sin^2\theta_\mu \cos^2\varphi_h)$
3	$\lvert A_\perp\rvert^2$	$\sin^2\theta_k(1 - \sin^2\theta_\mu \sin^2\varphi_h)$
4	$\lvert A_\parallel A_\perp\rvert$	$\sin^2\theta_k \sin^2\theta_\mu \sin 2\varphi_h$
5	$\lvert A_0 A_\parallel\rvert$	$\frac{1}{2}\sqrt{2}\sin 2\theta_k \sin 2\theta_\mu \cos\varphi_h$
6	$\lvert A_0 A_\perp\rvert$	$-\frac{1}{2}\sqrt{2}\sin 2\theta_k \sin 2\theta_\mu \sin\varphi_h$
7	$\lvert A_S\rvert^2$	$\frac{2}{3}\sin^2\theta_\mu$
8	$\lvert A_S A_\parallel\rvert$	$\frac{1}{3}\sqrt{6}\sin\theta_k \sin 2\theta_\mu \cos\varphi_h$
9	$\lvert A_S A_\perp\rvert$	$-\frac{1}{3}\sqrt{6}\sin\theta_k \sin 2\theta_\mu \sin\varphi_h$
10	$\lvert A_S A_0\rvert$	$\frac{4}{3}\sqrt{3}\cos\theta_K \sin^2\theta_\mu$

Results for S-wave components

$$
\begin{aligned}
|A_S^1|^2 &= 0.472 \pm 0.024 \pm 0.027, \\
|A_S^2|^2 &= 0.042\,^{+\,0.0013}_{-\,0.0009} \pm 0.010, \\
|A_S^3|^2 &= 0.0029\,^{+\,0.0013}_{-\,0.0009} \pm 0.023, \\
|A_S^4|^2 &= 0.0037\,^{+\,0.0025}_{-\,0.0019} \pm 0.032, \\
|A_S^5|^2 &= 0.0508\,^{+\,0.0070}_{-\,0.0019} \pm 0.027, \\
|A_S^6|^2 &= 0.151 \pm 0.011 \pm 0.051, \\
\delta_S^1 - \delta_\perp &= 2.05\,^{+\,0.12}_{-\,0.14} \pm 0.19\,\text{rad}, \\
\delta_S^2 - \delta_\perp &= 1.62\,^{+\,0.19}_{-\,0.19} \pm 0.41\,\text{rad}, \\
\delta_S^3 - \delta_\perp &= 1.16\,^{+\,0.37}_{-\,0.29} \pm 0.19\,\text{rad}, \\
\delta_S^4 - \delta_\perp &= -0.15\,^{+\,0.12}_{-\,0.15} \pm 0.31\,\text{rad}, \\
\delta_S^5 - \delta_\perp &= -0.637\,^{+\,0.068}_{-\,0.076} \pm 0.17\,\text{rad}, \\
\delta_S^6 - \delta_\perp &= -1.013\,^{+\,0.074}_{-\,0.083} \pm 0.07\,\text{rad}.
\end{aligned}
$$

Inputs for ϕ_s combination

Exp.	Mode	Dataset	$\phi_s^{c\bar{c}s}$	$\Delta\Gamma_s$ (ps^{-1})	Ref.
CDF	$J/\psi\,\phi$	$9.6\,fb^{-1}$	$[-0.60, +0.12]$, 68% CL	$+0.068 \pm 0.026 \pm 0.009$	[2]
D0	$J/\psi\,\phi$	$8.0\,fb^{-1}$	$-0.55^{+0.38}_{-0.36}$	$+0.163^{+0.065}_{-0.064}$	[3]
ATLAS	$J/\psi\,\phi$	$4.9\,fb^{-1}$	$+0.12 \pm 0.25 \pm 0.05$	$+0.053 \pm 0.021 \pm 0.010$	[4]
ATLAS	$J/\psi\,\phi$	$14.3\,fb^{-1}$	$-0.110 \pm 0.082 \pm 0.042$	$+0.101 \pm 0.013 \pm 0.007$	[5]
ATLAS	$J/\psi\,\phi$	$80.5\,fb^{-1}$	$-0.081 \pm 0.041 \pm 0.022$	$+0.0607 \pm 0.0047 \pm 0.0043$	[1]
ATLAS	above 3 combined		$-0.087 \pm 0.036 \pm 0.021$	$+0.0657 \pm 0.0043 \pm 0.0037$	[1]
CMS	$J/\psi\,\phi$	$19.7\,fb^{-1}$	$-0.075 \pm 0.097 \pm 0.031$	$+0.095 \pm 0.013 \pm 0.007$	[6]
CMS	$J/\psi\,\phi$	$96.4\,fb^{-1}$	$-0.011 \pm 0.050 \pm 0.010$	$+0.114 \pm 0.0014 \pm 0.0007$	[7]
CMS	above 2 combined		$-0.021 \pm 0.044 \pm 0.010$	$+0.1032 \pm 0.0095 \pm 0.0048$	[7]
LHCb	$J/\psi\,\phi$	$3.0\,fb^{-1}$	$-0.058 \pm 0.049 \pm 0.006$	$+0.0805 \pm 0.0091 \pm 0.0032$	[8]
LHCb	$J/\psi\,\pi^+\pi^-$	$3.0\,fb^{-1}$	$+0.070 \pm 0.068 \pm 0.008$	—	[9]
LHCb	$J/\psi\,K^+K^-$ [a]	$3.0\,fb^{-1}$	$+0.119 \pm 0.107 \pm 0.034$	$+0.066 \pm 0.018 \pm 0.010$	[10]
LHCb	$\psi(2S)\phi$	$3.0\,fb^{-1}$	$+0.23^{+0.29}_{-0.28} \pm 0.02$	$+0.066^{+0.41}_{-0.44} \pm 0.007$	[11]
LHCb	$D_s^+D_s^-$	$3.0\,fb^{-1}$	$+0.02 \pm 0.17 \pm 0.02$	—	[12]
LHCb	$J/\psi\,\pi^+\pi^-$	$1.9\,fb^{-1}$ [b]	$-0.057 \pm 0.060 \pm 0.011$	—	[?]
LHCb	$J/\psi\,\phi$	$1.9\,fb^{-1}$ [b]	$-0.083 \pm 0.041 \pm 0.006$	$+0.077 \pm 0.008 \pm 0.003$	[13]
LHCb	above 7 combined		-0.042 ± 0.025	$+0.0813 \pm 0.0048$	[13]
LHCb	$J/\psi\,\phi$ [c]	$3.0\,fb^{-1}$	$+0.00 \pm 0.28 \pm 0.07$	$+0.115 \pm 0.045 \pm 0.011$	[14]
$B_s^0 \to J/\psi\,\phi$ combined			-0.070 ± 0.022	$+0.074 \pm 0.006$	
All combined			-0.049 ± 0.019	$+0.077 \pm 0.006$	

[a] $m(K^+K^-) > 1.05$ GeV/c^2 [b] Run 2 [c] $J/\psi \to e^+e^-$

Control of penguin effects

LHCB-PAPER-2015-034

- Penguin effects estimated from $B_s^0 \to J/\psi K^{*0}$ and $B^0 \to J/\psi \rho^0$

$$\Delta\phi_{s,0}^{J/\psi\phi} = 0.000^{+0.009}_{-0.011}\,(\text{stat})\ {}^{+0.004}_{-0.009}\,(\text{syst})\ \text{rad}$$

$$\Delta\phi_{s,\parallel}^{J/\psi\phi} = 0.001^{+0.010}_{-0.014}\,(\text{stat}) \pm 0.008\,(\text{syst})\ \text{rad}$$

$$\Delta\phi_{s,\perp}^{J/\psi\phi} = 0.003^{+0.010}_{-0.014}\,(\text{stat}) \pm 0.008\,(\text{syst})\ \text{rad}$$

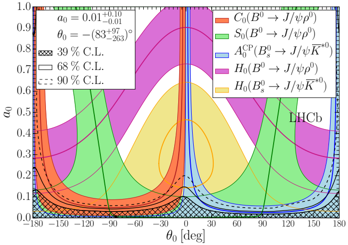

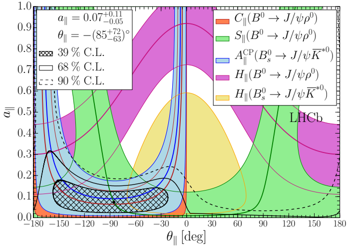

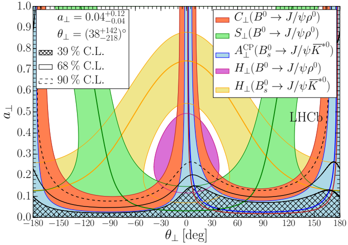

Validation check of ϕ_s in sub-samples

- Stable results in validation fits of various sub-samples
  - ✔ Magnet polarity
  - ✔ Trigger categories
  - ✔ Separate years
  - ✔ Bins of $p_T(B_s^0)$
  - ✔ Bins of $\eta(B_s^0)$
  - ✔ Separate tagging methods
  - ✔ number of primary vertices
  - ✔ PID variables
  - ✔ Different L0 triggers
  - ✔ Bootstrapping